NON-NEWTONIAN FLOW IN A CAVITY MIXER

P. Morris, K. Hourigan and M.C. Thompson
Fluid-dynamics Laboratory for Aeronautical and Industrial Research (FLAIR)
Dept. of Mechanical Engineering, Monash University, Clayton, Victoria

ABSTRACT

Many industrial fluids are non-Newtonian in nature. These fluids possess such properties as shear-thinning and thickening, plasticity and visco-elastic behaviour, to name but a few. Whilst many can be found in industrial mixing problems, there is no general way of finding the design variables that will lead to the most efficient mixing in any specific case. The current lack of knowledge means that there is little universality across the field, and that the costly process of studying each problem separately needs to be performed. For operating mixing vessels, design changes or different rheological properties can mean that the flow is far from optimal, and so the performance is badly degraded. Obviously a more systematic technique is required, and so the current work looks at the mixing of non-Newtonian fluids from a prototypical level to determine the main features and basic principles involved.

NOMENCLATURE

Cr	Carreau number
p	pressure
P	reduced pressure ($= p/\rho$)
Re	Reynolds number
S_{ij}	stress tensor
t	dimensionless time
$\mathbf{u}$	velocity vector
u_{top}	driving plate velocity
ρ	fluid density
ν_{eff}	effective fluid viscosity

1. INTRODUCTION

A large percentage of industrial liquids are non-Newtonian, such as polymer melts, slurries, suspensions and emulsions, paints and others. Efficient mixing of such materials is desirable at all levels of production, and cost obviously increases with the time and power input for the mechanical agitation, or a similar process, that is required. Minimisation of cost while still obtaining acceptable mixing quality is a major aim in any industrial situation. However, the current lack of understanding of the basic principles involved in both mixing and non-Newtonian fluids obviously delays any systematic techniques. Given that any fluid can be in a number of different states over a vast number of operating parameters and conditions, even within the same mixing vessel, finding the operational optimum can be an extremely difficult task. In the past, prediction of the flow patterns have been based on Newtonian theory (see Batchelor, 1967) with little modification. Whilst this may work in some simple cases, such as when the flow is only weakly shear-thinning or thickening, in visco-elastic flows, the flow direction may be completely reversed (Bowen *et al.*, 1991, Leong and Ottino, 1990).

Whilst complicated mixing vessels designs can be studied numerically, it is the ef-

fect of the fluid rheology on mixing that is studied presently. This has been done by removing most of the geometrical complexity and studying the flow in a cavity mixer. This basic prototype of a mixer has four walls which are allowed to move for certain periods of time. Tracer particles are seeded into the flow to give a measure of the performance and also mark regions where poor mixing occurs. Fluids with differing properties have been studied and compared with the Newtonian counterparts at equivalent conditions.

Section 2 looks at the mathematical formulation, while section 3 looks at the numerical scheme used in the current work. Results and a discussion of the mixing simulations are provided in section 4.

2. MATHEMATICAL FORMULATION

The formulation is based on the non-dimensionalised Navier-Stokes equations with adjustment for the viscosity changing with the flow shear rates. The governing equations are then

$$\frac{\partial \mathbf{u}}{\partial t} + (\mathbf{u}.\nabla)\,\mathbf{u} \;=\; -\nabla P \;+ \ldots$$

$$\frac{1}{Re}\left(\frac{\partial}{\partial x}\left(\nu_{eff}\frac{\partial \mathbf{u}}{\partial x}\right) + \frac{\partial}{\partial y}\left(\nu_{eff}\frac{\partial \mathbf{u}}{\partial y}\right)\right) \quad (1)$$

where P is pressure divided by the fluid density (p/ρ), $\mathbf{u} = (u, v)$, and ν_{eff} is the effective viscosity. The system is made consistent by the addition of the continuity equation

$$\nabla.\mathbf{u} = 0\,. \quad (2)$$

The effective viscosity, ν_{eff}, is given by the Carreau (1968) model with zero infinite-shear viscosity,

$$\nu_{eff} = \left(1 + (Cr)^2\dot{\gamma}^2\right)^{\frac{n-1}{2}} \quad (3)$$

where $\dot{\gamma} = \sqrt{\frac{1}{2}\Pi}, \Pi = S_{ij}S_{ij}$, and

$$S_{ij} = \frac{\partial u_i}{\partial x_j} + \frac{\partial u_j}{\partial x_i}\,. \quad (4)$$

Obviously the selection of $n = 1$ or $Cr = 0$ in (3) will lead to the standard Navier-Stokes form. Equation (3) is a preferred form for use in computations as it produces a finite value for the viscosity at any shear-rate, unlike the power-law models which have been used in the past. It also allows the establishment of a Reynolds number ($Re = UL/\nu_0$), based on the zero rate of shear viscosity, for comparison with the Newtonian counterparts.

The geometry used in the study has been simplified in order to delineate the effect of rheology on the flow patterns. The driven cavity flow is a well known test case of computational fluid dynamics (Ghia *et al.*, 1986), and serves as a basic prototype of a mixer. The system consists of a unit cavity where each wall is allowed to move in its own plane for certain periods of time in a prescribed fashion. Whilst all four walls can be driven to increase the mixing efficiency, in any real case this would be costly because some mechanical device is required to drive each. What is required is minimal amounts of agitation leading to the highest levels of mixing possible. Therefore, in the current study, only one of the four walls shall be driven in different fashions, and the others will remain stationary. A schematic of the design is shown in Figure 1.

3. NUMERICAL TECHNIQUE

Chaotic mixing simulations of the past (Souvaliotis *et. al.*, 1995) have demonstrated that small numerical errors may lead to false predictions within any computational simulation of mixing. Although the flows studied here are at a small enough Reynolds number that chaos should not appear, the code has been designed to handle this situation if it should occur. Therefore, the spatial variables are handled by a spectral expansion,

and the time stepping is handled by a high-order splitting scheme. As the flow is wall bounded, Chebyshev polynomials (Canuto *et al.*, 1988) are used in each direction within the flow. These are chosen because of the compression of the grid around the bounding walls when Gauss-Labotto points are used, and also the availability of a Fast Fourier Transform for derivative calculations. The time stepping is a modified version of the time-splitting used within spectral element simulations of the past (Karniadakis *et al.*, 1991). The convection terms are advanced first

$$\frac{\hat{\mathbf{u}} - \mathbf{u}^n}{\Delta t} = -(\mathbf{u}^n.\nabla)\mathbf{u}^n \qquad (5)$$

using an Adams-Bashforth scheme on the nonlinear term (see Press *et al.*, 1986). Continuity is then enforced on the following substep by a pressure projection

$$\frac{\hat{\hat{\mathbf{u}}} - \hat{\mathbf{u}}}{\Delta t} = -\nabla P. \qquad (6)$$

Finally, the diffusion step is performed with an implicit Crank-Nicholson discretisation

$$\frac{\mathbf{u}^{n+1} - \hat{\hat{\mathbf{u}}}}{\Delta t} = \frac{1}{2Re}\left(D_n\mathbf{u}^n + D_{n+1}\mathbf{u}^{n+1}\right) \qquad (7)$$

where the operator is given by

$$D_n = \frac{\partial}{\partial x}\left(\nu_n\frac{\partial}{\partial x}\right) + \frac{\partial}{\partial y}\left(\nu_n\frac{\partial}{\partial y}\right) \qquad (8)$$

As (8) contains a nonlinear implicit operator, this is handled in the current case via iteration. A linear diffusion term is added to both sides of (7) to form

$$\nabla^2\mathbf{u}_{iter+1} - \frac{2Re}{\Delta t}\mathbf{u}_{iter+1} = \nabla^2\mathbf{u}_{iter} - \frac{2Re}{\Delta t}\hat{\hat{\mathbf{u}}}\ldots$$

$$\ldots -(D_{iter}\mathbf{u}_{iter} + D_n\mathbf{u}_n)\ ,\ iter = 0, 1, \ldots \qquad (9)$$

which can be solved by standard explicit linear equation solvers (Canuto *et al.*, 1988). Iteration of (9) is performed until the changes in the velocity field are less than 10^{-9}. Although a spectral multigrid technique could be used in place here, the current technique requires little extra effort from a standard Navier-Stokes equation solver.

In order to establish the amount of mixing, passive particles are seeded into the flow and convected with the velocity field. A fourth-order Runge Kutta scheme is used to adjust the particle positions according to the equations

$$\frac{dx}{dt} = u \quad , \quad \frac{dy}{dt} = v. \qquad (10)$$

Initially, 25,000 particles are placed within the box at a position as shown in Figure 2. This is similar to the initial conditions used in Ottino (1989). However, given enough mixing time, the results become independent of the intial conditions.

4. RESULTS AND DISCUSSION

The numerical technique was first benchmarked on the driven cavity flow at a Reynolds number of 7500 for a Newtonian fluid. This provides a suitable test of the code, as results for this case are well published. At this Reynolds number, the flow lies close to the regime of transition to unsteadiness and false behaviour here due to spatial and temporal discretisation errors are easily detectable. Since a global spectral scheme is being used for the spatial variables, the driving lid velocity along the top wall cannot be uniform, but rather must approach zero at the corners. With the wall lying between $x \in (-1, 1)$, in the current study the velocity is given by

$$u_{top} = \left(1 - \exp(-50(1 - x^2))\right)^4. \qquad (11)$$

The fourth-order power on the right-hand side in (11) is used so that the higher derivatives of velocity are also zero at the corners. If the power is not used, then this leads to a discontinuity in vorticity

and hence problems with pressure boundary conditions (Karniadakis *et al.*, 1991). Figure 3 shows the calculated streamlines for this flow, in good agreement with Ghia *et al.* (1982) using a much higher resolution. A grid of size 65 × 65 was used in the present spectral scheme; however, doubling the grid size in both directions did not change the flow patterns and so the lower value will be used for all further simulations.

There are a number of free parameters and operating conditions available within the current study, the major ones being Re, Cr, n and the driving pattern on the top plate. An in-depth parameter search is not the aim of the current study, but rather to gain some understanding of the basic principles involved as shifts in values or patterns occur. The first case studied is that of Reynolds number dependency. A Newtonian fluid is considered initially, as they are relatively well understood. For high Reynolds numbers, the flow will be convectively dominated and so better mixing should occur at equivalent times. If the Reynolds numbers is indeed high enough, then chaotic velocity fields should result which will lead to even better mixing performance. Figure 4 shows four otherwise equivalent situations, except that Re has been changed in each. The driving pattern on the top lid is given by

$$u_{top} = \left(1 - \exp(-50(1 - x^2))\right)^4 (\sin(t))^2, \tag{12}$$

where t is the time. Differing driving patterns will be considered later; however, this one is known from experience to mix the particles significantly in a short time period. The figure shows each case at a non-dimensional time of $t = 100$, and the results are as expected. With the low Reynolds case, although the particles have generally moved westwards due to the driving pattern, only a small percentage of particles have been moved from the initial core. Slightly higher Re again leads to more movement and spreading; however, the particles do remain clumped around the initial starting position. Still higher values lead to much more mixing of the particles into the flow, and differing regions like chaotic islands (Ottino, 1989) can be seen to form. These are regions in which particles will not go, thus leading to voids in the mix. Time visualisations have revealed these to last only for certain periods of time, and then collapse and possibly form elsewhere.

The same Reynolds number dependency can also be established with the non-Newtonian flows. In any industrial case, the values of Cr and n in (3) would need to established from measurements of the actual fluid over a range of shear rates. The Reynolds numbers also tend to be lower with these flows due to the high zero-shear rate viscosities. In the present case, the values are arbitrary in order to establish generalised behaviour. Figure 5 shows the flow of a non-Newtonian fluid for two different Reynolds numbers, namely ten and one hundred, with the fluid having the values $n = 0.9$ and $Cr = 4$. The lower Reynolds number is seen to lead to poor mixing, with threads of particles merely forming a spiral within the cavity. The higher Reynolds case leads to significant mixing within the flow, although a denser central core of particles can still be seen.

Changes in the parameters for the non-Newtonian viscosity in (3) are considered next, to determine the flow dependency. Figure 6 shows the flow with $Re = 100$, $n = 0.9$, and one value of Cr double the other. At this Reynolds number, the patterns are near identical, except for some core deformation. Thus the conclusion is that slight changes in this parameter do

not affect results greatly. Changes in the value of n can also be seen to produce similar results in Figure 7, where $Re = 10$, $Cr = 4$, and the value of n is increased. It thus appears that the Reynolds number dependency is the strongest in these flows.

Finally, the effect of the plate driving pattern on the degree of mixing is considered. The non-Newtonian parameters are set to $Cr = 4$ and $n = 0.7$, and the Reynolds number is equal to ten. Although many analytic forms have been suggested in the past (Ottino, 1989), only four shall be studied here, these being

$$u_{top} = (1 - \exp(-50(1 - x^2)))^4 \tanh(t)$$
$$u_{top} = (1 - \exp(-50(1 - x^2)))^4 \sin(t)$$
$$u_{top} = (1 - \exp(-50(1 - x^2)))^4 (\sin(t))^2$$
$$u_{top} = (1 - \exp(-50(1 - x^2)))^4 |\sin(t)|$$

The first is just the driven cavity profile with a time lag to allow for a smooth change from the zero initial condition. The other three contain a periodical component, but each can have a different value or sign at the same time.

Figure 8 shows the particle positions for each driving pattern at equivalent times, $t = 125$, and the differences are clear. The *tanh* driving pattern merely drives the fluid in a single direction, and after the initial start-up, at a uniform velocity. The spiral threads of particles seen around the central core tend to closely follow the streamlines (see Figure 3). This is not surprising, as the flow is steady at this Reynolds number after this time evolution. The *sin* dependence leads to the least spreading of the particles within the flow, mainly because as the core is moved in one direction in a half-period, it is then returned back to a similar starting position as the velocities are reversed in the next half. The distortion is due to the diffusion and the particle positions never quite returning to the initial values. Therefore it is to expected that if the plate is driven in one direction only, then the amount of mixing within the flow may be improved. Both the last two profiles have this feature, but it must be remembered that the sin^2 profile will have lower velocities over most of the period compared to the other. The two spiral patterns look similar, however, the $|sin|$ profile has allowed extra particle movement from the denser core. This core of particles appears to have only been stretched slightly in the sin^2 case.

5. CONCLUSIONS

Mixing behaviour in non-Newtonian flows has been studied with the use of a prototypical cavity mixer. This has allowed comparison with Newtonian flows, thus establishing the changes caused by fluid rheology alone. Although driving the four walls in a certain pattern or in a random manner may lead to substantial mixing, the realisation is that in any industrial situation the wall motion must be driven by a mechanical device and so adding to the cost of production. Therefore, improvements in mixing with a minimum amount of mechanical agitation is the aim.

The numerical scheme used was a global spectral technique with iteration for the non-linear viscosity at every timestep. This effectively overcomes the difficulties with linearisation techniques used in global spectral schemes of the past, and has further extensions to large eddy simulation modelling of turbulence. The high-order temporal and spatial scheme can be further generalised to include more complicated viscosity models, such as a visco-elastic type (Oldroyd, 1964), but shall await a further study.

ACKNOWLEDGEMENTS

The financial assistance from the Monash

University Research Fund for this project is gratefully acknowledged.

REFERENCES

Batchelor, G.K. (1967). An introduction to fluid dynamics. Cambridge University Press, Sydney, 615pp.

Bowen, P.J., Davies, A.R. and Walters, K. (1991). On viscoelastic effects in swirling flows. J. Non-Newtonian Fluid Mech., **38**, 113-126.

Canuto, C., Hussaini, M.Y., Quarteroni, A. and Zang, T.A. (1988). Spectral methods in fluid dynamics. Springer-Verlag.

Carreau, P.J. (1968). Rheological equations from molecular network theories. Ph.D thesis, Univ. Wisconsin, Madison.

Ghia, U., Ghia, K.N. and Shin, C.T. (1982). High-Re solutions for incompressible flow using the Navier-Stokes equations and a multigrid method. J. Comp. Phys., **48**, 387-411.

Karniadakis, G.E., Israeli, M. and Orszag, S.A. (1991). High-order splitting methods for the incompressible Navier-Stokes equations. J. Comp. Phys., **97**, 414-443.

Leong, C.W. and Ottino, J.M. (1990). Increase in regularity by polymer addition during chaotic mixing in two-dimensional flows. Phys. Rev. Lett, **64**, 874-877.

Oldroyd, J.G. (1964). *In* Second-order effects in elasticity, plasticity and fluid mechanics. Ed M. Reiner and D. Abir, 520-529, Macmillan, New York.

Ottino, J.M. (1989). The kinematics of mixing: stretching, chaos, and transport. Cambridge University Press, Sydney, 364pp.

Press, W.H., Flannery, B.P., Teukolsky, S.A. and Vetterling, W.T. (1986). Numerical Recipes. Cambridge University Press, Melbourne, 818pp.

Souvaliotis, A., Jana, S.C. and Ottino, J.M. (1995). Potentialities and limitations of mixing simulations. AIChE, **41**, 1605-1621.

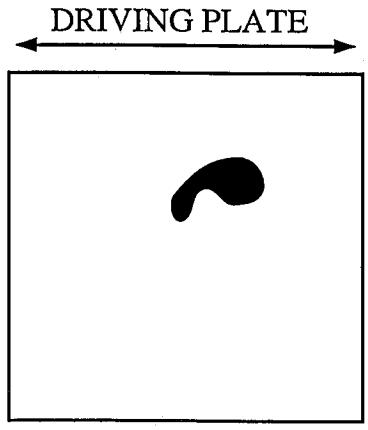

Figure 1. Schematic of the cavity mixer design.

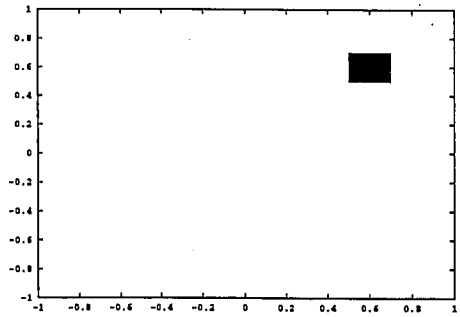

Figure 2. Initial particle positions.

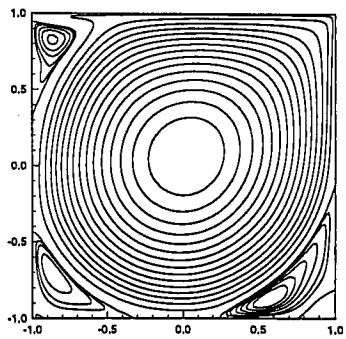

Figure 3. Driven cavity flow at Re=7500.

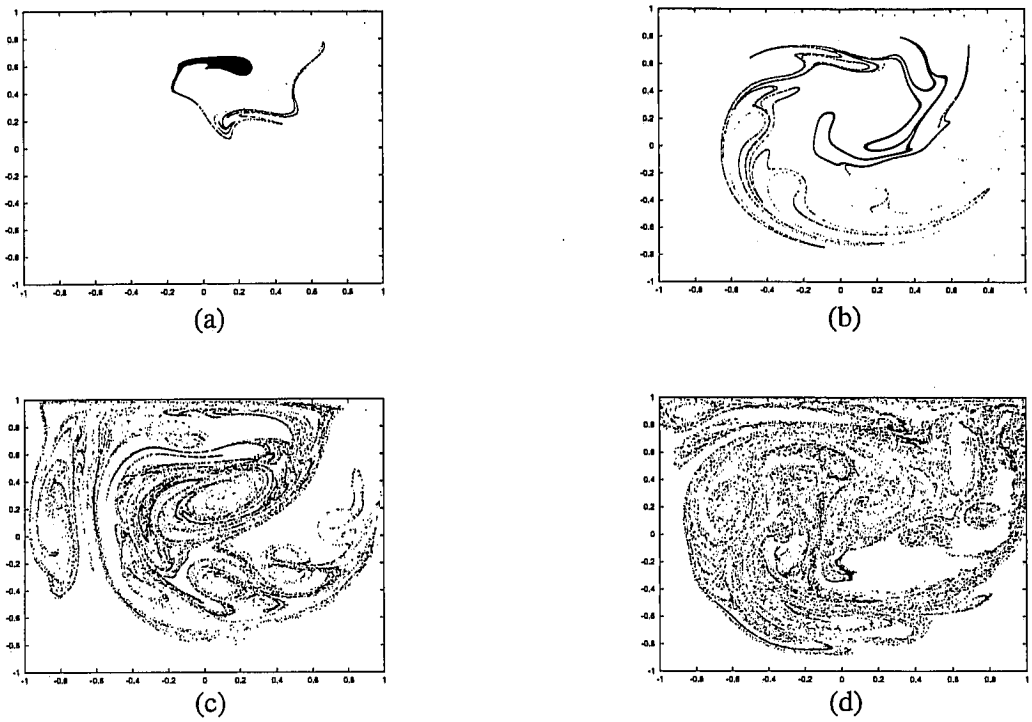

Figure 4. Particle distributions within the cavity at $t = 125$ and four different Reynolds numbers, (a) Re=100, (b) Re=1000, (c) Re=10000, (d) Re=20000.

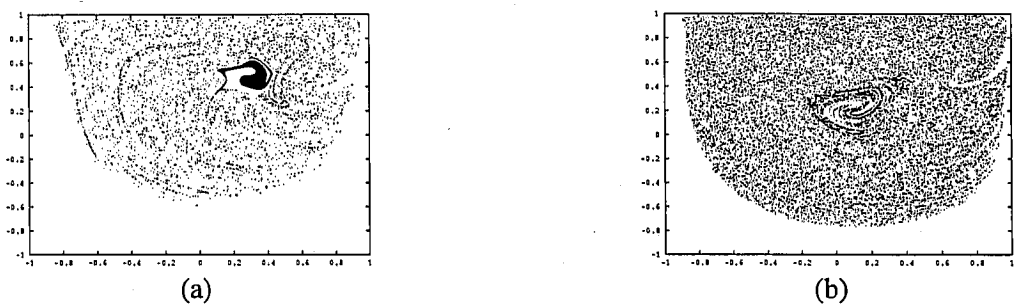

Figure 5. Particle distributions for a non-Newtonian fluid ($n = 0.9, Cr = 4$), and (a) Re=100, (b) Re=500.

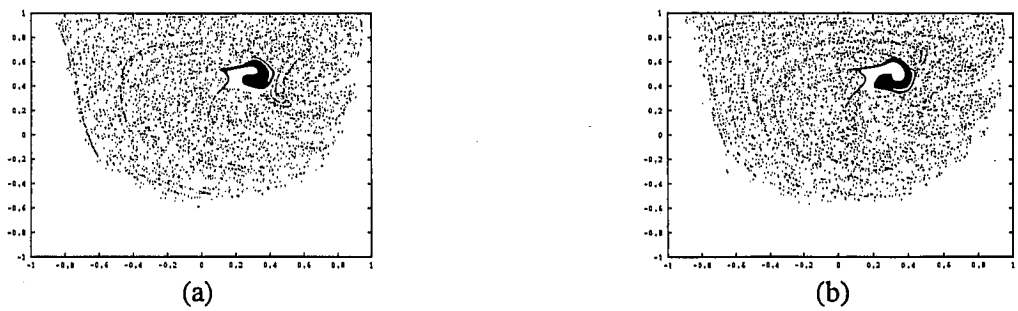

Figure 6. Particle distributions at $t = 125$ with $n = 0.9$, $Re = 100$ and (a) $Cr = 4$, (b) $Cr = 8$.

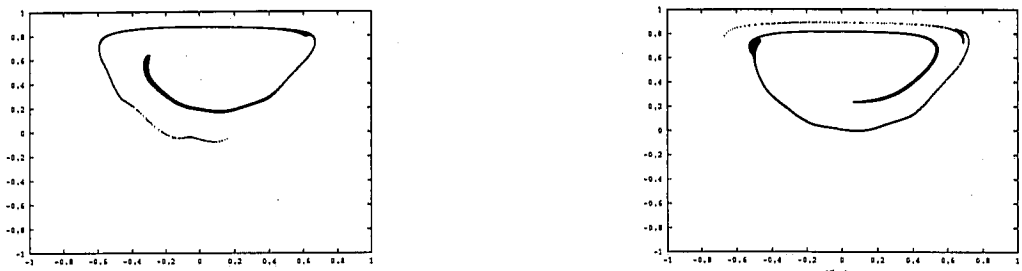

Figure 7. Particle distributions with $Cr = 4$, $Re = 10$, and (a) $n = 0.7$, (b) $n = 0.9$.

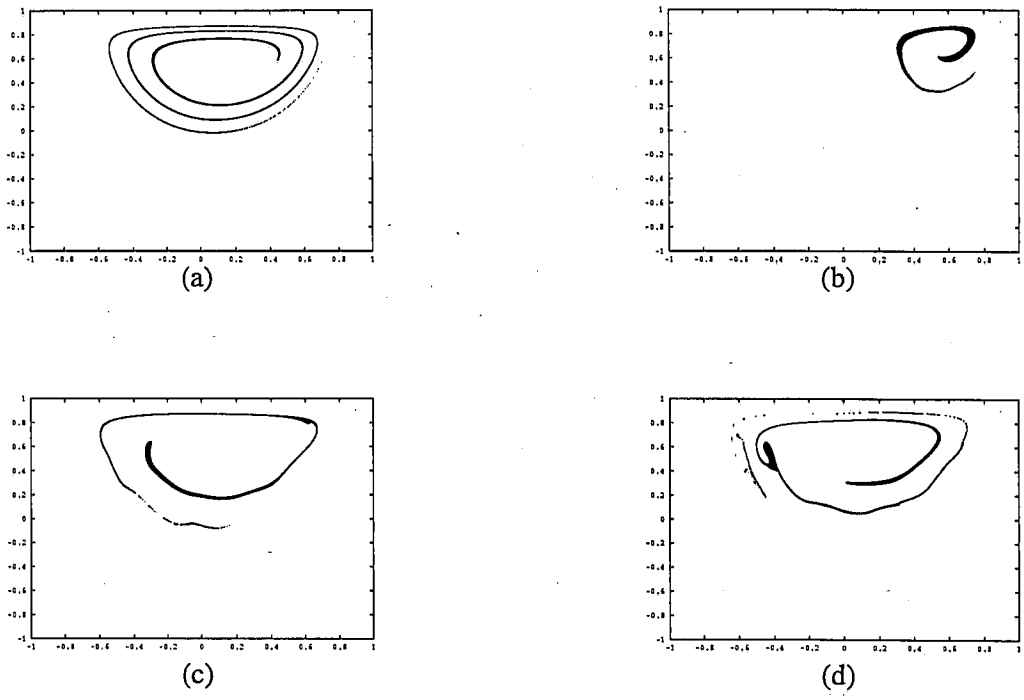

Figure 8. The effect of the plate driving pattern on non-Newtonian mixing.
(a) $u_{top} = F(x)tanh(t)$, (b) $u_{top} = F(x)sin(t)$
(c) $u_{top} = F(x)sin^2(t)$, (d) $u_{top} = F(x)|sin(t)|$,
where $F(x) = (1 - exp(-50(1 - x^2)))^4$.